Thin Solid Films 636 (2017) 384–391

Contents lists available at ScienceDirect

Thin Solid Films

journal homepage: www.elsevier.com/locate/tsf

# Preferential orientation in bismuth thin films as a function of growth conditions

S.E. Rodil [a,*], O. Garcia-Zarco [a], E. Camps [b], H. Estrada [c], M. Lejeune [d], L. Bourja [d], A. Zeinert [d]

[a] Instituto de Investigaciones en Materiales, Universidad Nacional Autónoma de México, Mexico, Circuito Exterior s/n, CU, México D.F. 04510, Mexico
[b] Departamento de Física, Instituto Nacional de Investigaciones Nucleares, Apartado Postal 18-1027, México D.F. C.P. 11801, Mexico
[c] Centro de Ingeniería y Desarrollo Industrial, Av. Playa Pie de la Cuesta No. 702, Desarrollo San Pablo, C.P. 7612, Santiago de Querétaro, Qro, Mexico
[d] Laboratoire de Physique de la Matière Condensée, Université de Picardie Jules Verne, 33 rue St. Leu, 80039 Amiens, France

ARTICLE INFO

*Article history:*
Received 13 January 2017
Received in revised form 19 June 2017
Accepted 24 June 2017
Available online 26 June 2017

*Keywords:*
Bismuth
Sputtering
Pulsed laser deposition
Electron beam evaporation
Thermal evaporation
Thin films
Growth

ABSTRACT

Bismuth thin films are known to exhibit interesting properties that can be explored for new applications such as optical or electrical sensors and thermoelectric devices. Due to the large anisotropy of the electronic band structure of Bi, its conductivity and optical functions are largely dependent on the preferred orientation obtained for the polycrystalline thin films, which are determined by the deposition system and the parameters.
In this study we report on the growth of bismuth thin films deposited by various deposition methods, all of them starting from the vapor phase but with different energies associated to the impinging species: thermal and electron beam evaporation, direct and alternating current magnetron sputtering, and pulsed laser evaporation. It is shown that the texture developed in Bi thin films follows a competitive growth texture in which the crystallographic planes with lower surface energy are favored and this process is dominant unless enough energy is supplied either by substrate heating or high energy bombardment.



## 1. Introduction

Studies about the synthesis and properties of bismuth thin films is an old subject [1–13], however the deposition of high quality films is still a challenge. Bismuth is a semimetal presenting a small overlap between the bottom of the conduction and the top of the valence bands, so the density of states at the Fermi level is negligible. For the semimetals, both electron and holes contribute to the conductivity, leading to a different conductivity vs. temperature dependence than metals. Particularly, Bi exhibits a strong temperature and magnetic field dependence of the electrical resistance, which might be useful for magnetic field sensing applications [14]. Moreover, Bi also presents one of the largest Seebeck coefficients that has been studied numerous times [15,16] and nevertheless, there is a serious discrepancy about the temperature dependence of the Seebeck coefficient of bismuth both in the bulk and thin-film state [15]. As a thin film, Bi exhibited quantum size confinement effects [16–20], such as anomalous electronic transport properties [9,17]. As described by Condurache-Bota et al. [21] this is considered to be due to the quantization of the component of the electron momentum normal to the film plane, which theoretically should lead to a decrease and even to the disappearance of the overlap between the valence and the conduction bands. This predicts that a semimetal-to-semiconductor transition should occur for thickness in the 20–30 nm range [1,5,9,22–24]. However, even after many years of this prediction, the experimental results are still controversial [24–26]. In a recent paper, one of the possible explanations for the discrepancies is related to the surface quality of the films [27], while in another study the differences are related to the texture (preferential crystal orientation growth) of the films [12,28].

One characteristic of the bismuth band structure is that it is highly anisotropic [29–31], then most of the electron, optical and thermal transport properties are also anisotropic [12,32–35]. However, the effect of such anisotropy has not been considered to explain the discrepancies in the properties of Bi thin films measured by different groups [15]. This is even more relevant considering that the Bi thin films present a high degree of preferential orientation growth into the (003) direction (hexagonal crystallographic system, which is equivalent to the (111) direction in the rhombohedral crystallographic system), such texture has been observed for different growth systems, deposition conditions and substrates [12,26,33,36–41]. Nevertheless, few works also report the growth into the (012) direction [42,43] or random orientation [44,45], but there is not a clear explanation for the variation in the film texture.

The aim of the present work is to identify different experimental parameters that lead to variations in the texture or preferred orientation of bismuth thin films. Such parameters have been investigated for three deposition systems: evaporation, sputtering and pulsed laser deposition, aiming to find a fundamental parameter that could explain the large variation that has been observed experimentally. This texture

* Corresponding author.
*E-mail address:* srodil@unam.mx (S.E. Rodil).

http://dx.doi.org/10.1016/j.tsf.2017.06.048
0040-6090/

variation in such a high anisotropic material could partially explain the discrepancies on the electronic and transport properties of the Bi thin films.

## 2. Experimental procedure

### 2.1. Film deposition

Bi thin films were grown on silicon (100) or glass substrates using three different deposition methods: magnetron sputtering, evaporation and pulsed laser deposition (PLD). For each technique some variations were also introduced such as radio frequency or direct current for sputtering; E-beam or thermal evaporation or the ion energy during the PLD process.

#### 2.1.1. Sputtering

*2.1.1.1. Direct current.* Bismuth thin films were prepared at room temperature by a DC magnetron sputtering technique of high purity bismuth target (4″) and an inert gas (Ar: 10 sccm) onto silicon Si(100) and glass substrates. The base pressure of the deposition chamber was $1.4 \times 10^{-4}$ Pa and the working pressure was set at 4 Pa. A thickness-series was produced; from about 10 nm to 1400 nm by a combination of increasing the deposition time from 30 to 600 s and the current applied to the target, as indicated in Table 1.

*2.1.1.2. Radio frequency.* Bismuth thin films were prepared at room temperature by the RF magnetron sputtering technique of high purity bismuth target (4″) and an inert gas (Ar) onto silicon Si(100) and glass substrates. The base pressure of the deposition chamber was $6 \times 10^{-4}$ Pa and the working pressure was set at 4 Pa. In order to obtain films with different thicknesses, the films were prepared using radio frequency powers of 45 and 60 W and deposition times between 1 and 15 min, as described in Table 2.

#### 2.1.2. Evaporation

For evaporation two different systems were used. One normal thermal evaporator with a fixed filament-substrate distance; 10 films with different deposition times were deposited at fixed current (20 A) and vacuum conditions ($1.0 \times 10^{-3}$ Pa). On the other hand, the other system was an electron beam evaporator with a variable source-substrate distance. In such case, three samples were produced increasing the thickness by varying the filament-substrate distance from 12 to 75 cm, but keeping all the other conditions fixed (Table 3). Films were deposited onto glass substrates.

**Table 1**
Deposition conditions and thickness of the samples deposited by DC-sputtering.

| Sample name | Current (A) | Time (s) | Thickness (nm) ±5% |
|---|---|---|---|
| DC1-1 | 0.1 | 30 | 12 |
| DC1-2 | 0.1 | 50 | 27 |
| DC1-3 | 0.1 | 70 | 57 |
| DC1-4 | 0.1 | 90 | 62 |
| DC1-5 | 0.1 | 300 | 186 |
| DC2-1 | 0.2 | 50 | 118 |
| DC2-2 | 0.2 | 90 | 173 |
| DC2-3 | 0.2 | 300 | 449 |
| DC2-4 | 0.2 | 600 | 1394 |

**Table 2**
Deposition conditions and thickness of the samples deposited by RF-sputtering.

| Sample name | RF power (W) | Time (s) | Thickness (nm) ±5% |
|---|---|---|---|
| RF1-1 | 45 | 300 | 604 |
| RF1-2 | 45 | 600 | 1200 |
| RF2-1 | 60 | 600 | 170 |
| RF2-2 | 60 | 900 | 2262 |

**Table 3**
Deposition conditions and thickness for the samples deposited by evaporation.

| Sample name | Time (s) | Distance (cm) | Thickness (nm) ±5% |
|---|---|---|---|
| Th1 | 5 | 3 | 71 |
| Th2 | 15 | 3 | 75 |
| Th3 | 25 | 3 | 150 |
| Th4 | 40 | 3 | 287 |
| Th5 | 80 | 3 | 474 |
| Th6 | 180 | 3 | 2029 |
| Ebeam1 | 100 | 75 | 180 |
| Ebeam2 | 100 | 25 | 500 |
| Ebeam3 | 100 | 12 | 850 |

#### 2.1.3. Pulsed laser deposition

Ablation was carried out using a Nd:YAG laser with emission at the fundamental line, 5 ns pulse duration, 10 Hz repetition rate and 500 mJ maximum output energy. The laser beam was focused on a Bismuth target (99.98%) at an incident angle of 30° with respect to the surface normal. The target was rotating at 15 rpm, in order to avoid laser drilling. The working chamber was evacuated to a base pressure of $1.4 \times 10^{-4}$ Pa. The vacuum chamber was baked at 100 °C for 20 min in order to reduce the residual humidity, and thus the possible contamination of the samples during deposition.

Two sets of samples were deposited using the mean kinetic Bi ion energies as the key parameter (Table 4). The first one called PLD1 is a group of samples deposited using an average ion energy around 110 eV (also called low energy, LE), the second one called PLD2, is a group of samples deposited using an average ion energy around 270 eV (also called high energy, HE). Different deposition times were used to obtain different thicknesses (Table 4). The ion energy selection was done using a Langmuir planar probe. This is a technique currently used in many facilities working with PLD (see for example [46] and references cited there in). The probe is located at the substrate position, and removed after the plasma parameters were measured. The probe consisted of a 6-mm diameter stainless steel disk, biased to a fixed voltage at −50 V, where saturation of the ion current was evident. The signal from the probe was monitored through a 15 Ω load resistor and recorded on a fast digital oscilloscope. From the Time of Flight (TOF) curves it was possible to obtain the mean kinetic ion energy following the procedure described in Ref [47]. The accuracy of the method gives us standard deviation around 10%, which is reflected in the small variation in the ion energy for each group. The ion energy values are the result of the combination of various experimental parameters; the substrate-target distance and the applied fluence, therefore the probe is required to set the conditions that lead to the desired ion energy

**Table 4**
Deposition conditions and thickness of the samples deposited by pulsed laser deposition.

| Sample name | Bi ion energy (eV) ±10 eV | Deposition time (min) | Thickness (nm) ±5% |
|---|---|---|---|
| PLD1-1 | 120 | 4 | 20 |
| PLD1-2 | 100 | 15 | 54 |
| PLD1-3 | 103 | 20 | 110 |
| PLD1-4 | 118 | 30 | 150 |
| PLD1-5 | 113 | 40 | 200 |
| PLD1-6 | 110 | 60 | 600 |
| PLD2-1 | 260 | 15 | 60 |
| PLD2-2 | 270 | 25 | 100 |
| PLD2-3 | 280 | 40 | 200 |
| PLD2-4 | 270 | 60 | 800 |

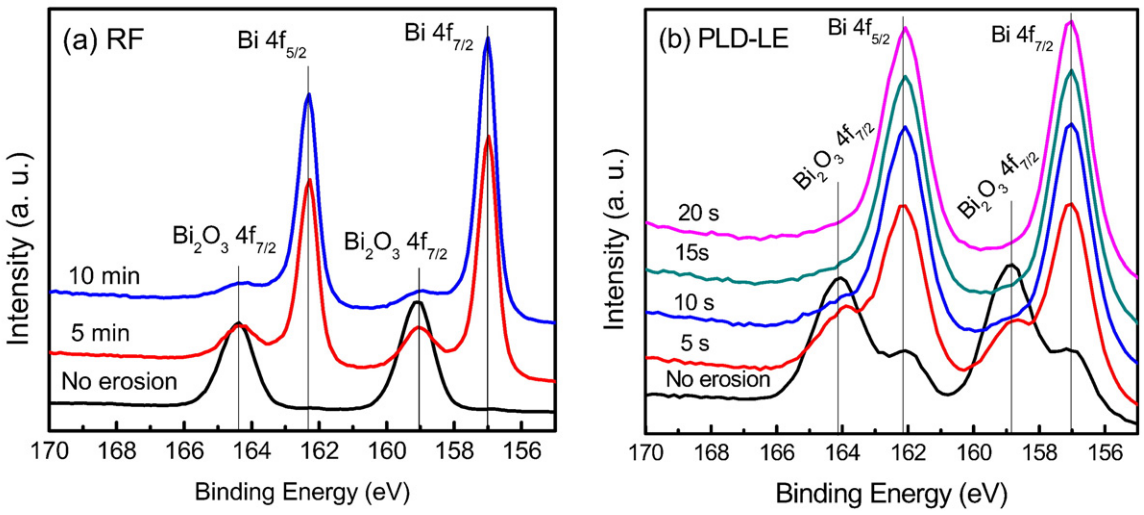


**Fig. 1.** Evolution of the Bi photoelectron peak as a function of the erosion time for (a) RF1-1 and (b) PLD1-6 samples.

value. The target to substrate distance was set at 5 cm and the fluence delivered to the target for the low energy samples was between 0.81 and 0.85 J/cm$^2$, while for the high energy deposition, the fluence was between 2.7 and 3.0 J/cm$^2$. Bismuth thin films were deposited at room temperature at the base pressure on 1.5 × 1.5 cm pieces of Pyrex glass.

The values of the ion energy were selected in terms of the aim of the present study. Ion energies far from 110 ± 10 eV or 270 ± 10 eV produced polycrystalline films without a well-defined preferred orientation, while much higher energies lead to drastic target damage.

### 2.2. Film characterization

For all the systems, the film deposition rate was evaluated adding a mask during the deposition, so that the height of the step could be measured by profilometry (KLA D120 Tencor or Dektak III profilometer). The reported results are the average of at least 10 measurements with a maximum standard deviation of 5%.

The composition of the films was confirmed using energy dispersive spectroscopy (EDS) coupled to a scanning electron microscope (SEM) and X-ray photoelectron spectroscopy (XPS).

The film structure was evaluated using X-ray diffractometer (Rigaku Ultima IV) using the thin film attachment and parallel beam but in the θ–2θ configuration in order to obtain a good X-ray penetration and study the average structure of the films and not only the outer-layers. The XRD patterns were normalized to consider the different thickness of the samples. The preferred orientation coefficient or texture coefficients were estimated using Eq. (1) from reference [48].

$$TC_{hkl} = \frac{\frac{I^{meas}_{hkl}}{I^{o}_{hkl}}}{\frac{1}{N}\sum_{h'k'l'}\frac{I^{meas}_{h'k'l'}}{I^{o}_{h'k'l'}}} \quad (1)$$

where $I^{meas}_{hkl}$ is the measured intensity of each (hkl) peak, $I^{o}_{hkl}$ is the theoretical relative intensity provided by the XRD reference data (JCPDS 85-1331). Finally, N is the number of reflections considered from all the different samples. The maximum number of reflections used for the estimation of the texture coefficient was N = 4, since the more commonly obtained peaks were: (003), (012), (104) and (101). This means that the texture coefficient will be between 0 and 4, where 4 indicates a highly textured sample, 1 a randomly oriented sample and 0 no observation of that peak. It is important to mention that the pseudo-cubic notation for the Bi structure has been used.

## 3. Results

The growth rate is strongly dependent on the deposition conditions of each system, but in comparison to other metallic films, it is relatively high for all the deposition methods. The films composition analysis indicated the formation of pure Bi films without other contaminants, except

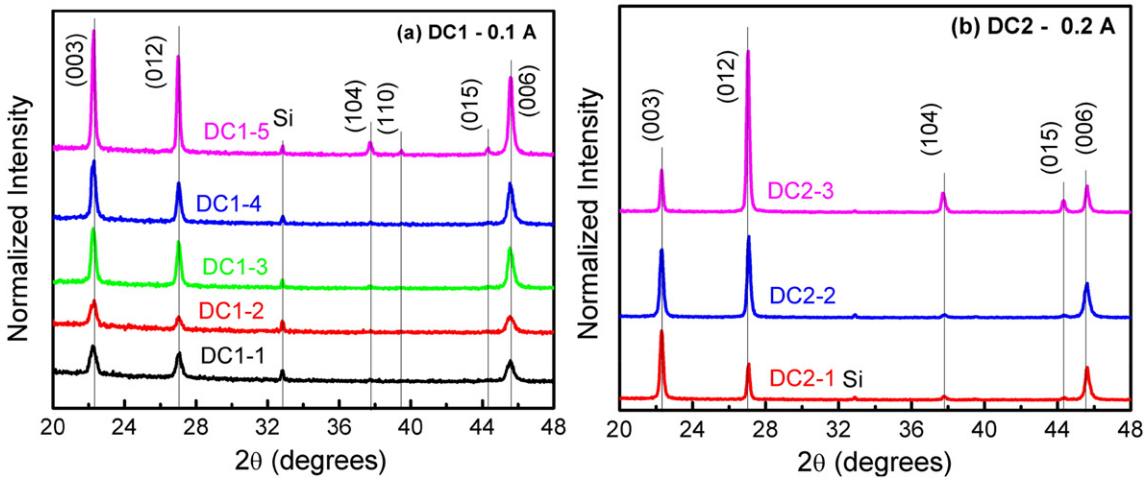


**Fig. 2.** X-ray diffraction patterns of the Bi thin films deposited by DC magnetron sputtering.

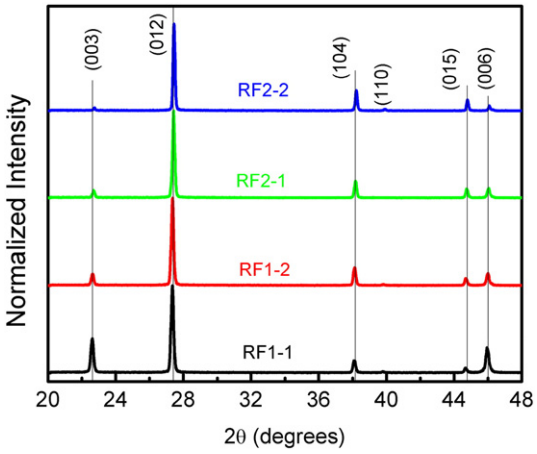


**Fig. 3.** X-ray diffraction patterns for the samples deposited using RF magnetron sputtering.

for a very thin $Bi_2O_3$ thin layer formed on the surface, as can be observed in the photoelectron spectra shown in Fig. 1. The XPS analysis was done for different samples and Fig. 1 shows only two examples for RF-sputtered and a PLD-LE samples. The surface cleaning was done using different conditions for the Ar ion beam source; the PLD sample was cleaned using 3 kV, 10 μA, while for the sputtered sample less energetic conditions were used: 2 kV, 2 μA. Nevertheless, for both samples the oxide layer was completely removed. Estimation of the oxide layer thickness was not done, since the erosion rate is highly dependent on the Ar ion energy and current and, calculations based on the relative integrated intensities required knowledge of the inelastic mean free paths for electron scattering in both Bi and $Bi_2O_3$ [49]. However, assuming that the maximum escape depth for photoelectrons is about 10 nm [50], Fig. 1(a) for the sputtered sample suggests that the oxide layer was thicker than 10 nm since no metallic Bi signal is detected. However, for the PLD sample (Fig. 1(b)), the spectrum without erosion shows contribution from both chemical states; $Bi^0$ and $Bi_2O_3$ indicating that the oxide layer is thinner than 10 nm. Growth of a native oxide layer on Bi thin films has been observed before by Atkinson and Curran [51], who estimated, by spectroscopic ellipsometry, that the thickness of the layer after 9 days of exposure to air was about 1.6 nm. A similar work was done by de Sande et al. [52] comparing the thickness of the Bi oxide layer on sputtered and PLD deposited Bi films after storage at room temperature and atmospheric conditions for a six month period. Their results suggest that the oxide layer grows slowly on the PLD films in comparison to both sputtered and the evaporated films from Atkinson and Curran [51], nevertheless, the oxide thickness reached about 2 nm after 2 months, which is much thinner than the estimation given above for the films reported in the present work. In both papers [51, 52], the estimation of the $Bi_2O_3$ thickness was done using the Bi dielectric functions (and also the $Bi_2O_3$ refractive index) estimated from previous works. However, more recently Toudert et al. [33] have shown that there are many discrepancies between the reported dielectric functions of Bi due to certain artifacts, such as porosity or roughness that were not properly taken into account, therefore it is likely that the native oxide thickness estimation was also not correct.

The normalized XRD patterns for the DC sputtered samples are shown in Fig. 2a, b. For the DC1 series (0.1 A), the same pattern is observed as the thickness increased from 11.6 to 185.6 nm. The samples show a polycrystalline structure, showing diffraction peaks from the (003), (012), (104), (110), (015) and (006) planes. The intensity of the (003) peak is larger or comparable to the (012) peak which is a clear indication of a (003) preferred orientation since according to the reference powder data (JCPDS 85-1331) its intensity should be only 5% of the main peak (012). The DC2 thicker samples (0.2 A) presented also predominantly the (003), (012), (104), (015) and (006) peaks. As the thickness increased from 118.2 to 448.5 nm, the relative intensity between (003)/(012) peaks was clearly reversed; the thicker the samples, the lower the (003) intensity.

Fig. 2 shows the diffraction patterns of the samples deposited on Si substrates, but identical patterns were also obtained for the glass substrates, suggesting that under the deposition conditions used, the substrate has no effect on the crystalline structure of the Bi films. A similar behavior was observed by Stanley et al. [45] for sputtered deposited films.

Fig. 3 shows the XRD patterns obtained for the Bi thin films deposited by magnetron sputtering using an RF power supply. The reflections (003), (012), (104), (110), (015) and (006) are observed. For these thicker samples, the intensity of the (003) peak is always lower than the (012) peak and indeed the (003)/(012) intensity ratio decreases as the thickness increased. Similar patterns were also reported by Kim et al. [44] for Bi thin films grown using RF-sputtering.

Fig. 4a, b shows the diffraction patterns for the thermal and E-beam evaporated samples. For the thinner (70–287 nm) thermal evaporated samples, the films presented a purely (003) oriented diffraction pattern (only (003 and (006) reflections are observed), as has been reported previously for evaporated Bi films [12,15]. However as the thickness increased, other diffraction families are shown (012), (101), (104) and (110). So, for the thicker sample (2029 nm), both (003) and (012) peaks presented comparable intensities and nevertheless, the high value for the (003) peak indicates yet a preferential (003) orientation.

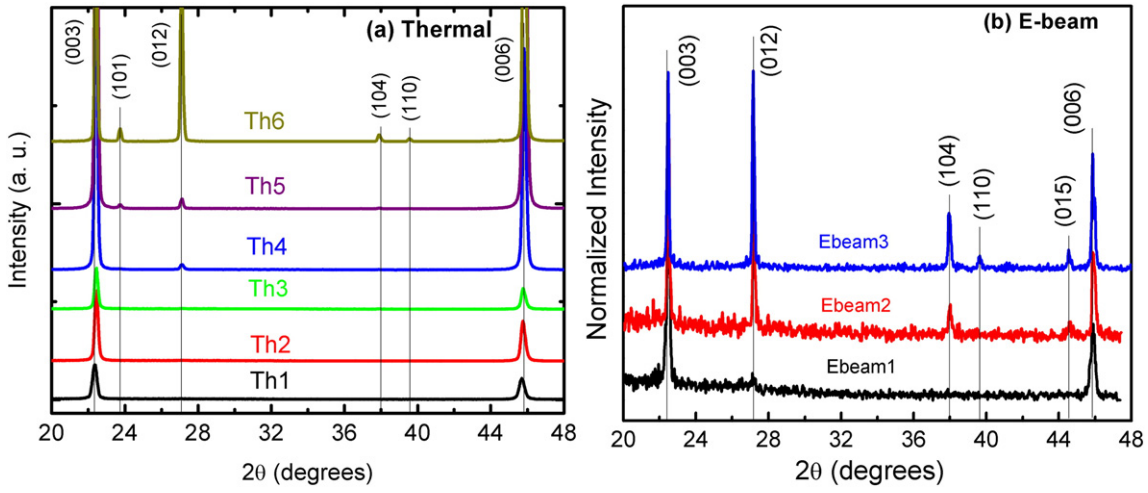


**Fig. 4.** X ray-diffraction patterns of the Bi thin films deposited by evaporation (a) Thermal evaporator as a function of the deposition time; the patterns were not normalized and (b) E-beam evaporator as a function of the source-substrate distance.

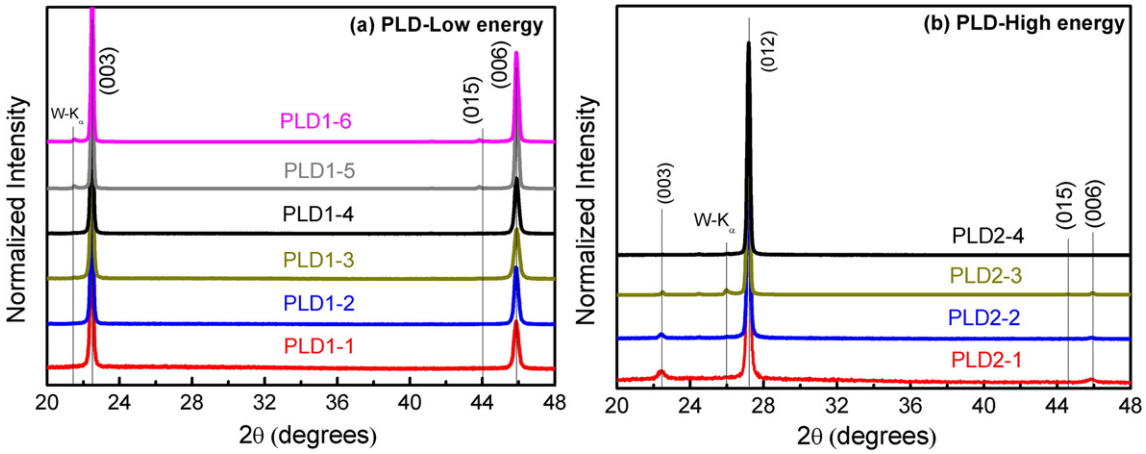


**Fig. 5.** X-ray diffraction patterns of the Bi thin films deposited by pulsed laser ablation using (a) low ionic energy (~110 eV) and (b) high ionic energy (~270 eV).

A similar trend is also obtained for the E-beam samples; the thinner samples shows only (003) family peaks, but as the thickness increased the (012) signal grows-up.

Fig. 5a, b shows the XRD patterns for the PLD samples, where a large difference between the two sets can be observed. The low energy samples have a pure (003) orientation, which has also been shown for other PLD films [33], while the high energy presented a (012) preferential orientation, not so commonly observed.

The XRD patterns were analyzed to estimate the (003) preferred orientation using the texture coefficient defined in Eq. (1). Fig. 6 shows the (003) texture coefficient for the different samples as a function of the films thickness.

Fig. 6 clearly showed that for evaporation and low energy PLD, it is possible to keep the (003) as the preferred orientation for thickness above 600 nm; for E-beam, it was possible to grow a 2 μm thick film showing the (003) texture. However, when sputtering is used, either DC or RF, the trend indicates that the purely preferred (003) orientation can be maintained only at thickness below <200 nm or equivalent short deposition times. As the films become thicker, the $TC_{(003)}$ decreased and the texture coefficient reaches unity, meaning a random orientation. The high-energy deposited PLD films showed a completely different behavior. None of the films showed a preferred (003) orientation ($TC_{(003)}$ < 4) and as the thickness increased the presence of the (003) reflection is completely lost. The XRD patterns shown in Fig. 5 indicated that the texture changed to a predominantly (012) orientation. Using PLD and high ion energy (~280 eV), it was possible to obtain nearly pure (012) preferred orientation, not attained with any of the other deposition systems.

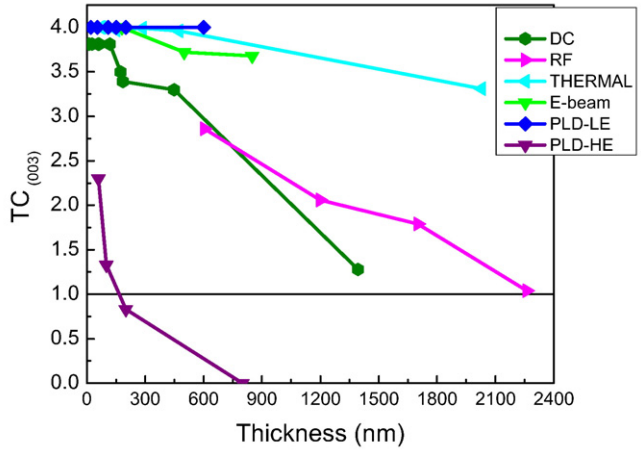


**Fig. 6.** Value of the texture coefficient for the (003) orientation as a function of the film thickness. $TC_{(003)}$ equal to 4 means unique orientation, $TC_{(003)} = 1$ means random orientation as in a powder samples and $TC_{(003)} = 0$ indicates that no (003) peak is observed.

The differences in surface morphology and texture were also evident by observing the films by SEM, as can be observed in Fig. 7. The evaporated-pure (003) oriented sample shows an ordered arrangement of the crystals, where a high fraction of them present a triangular shape, characteristic of an hexagonal crystal oriented with the c-axis perpendicular to the substrate, as has been observed by other authors using atomic force microscopy [53–55].

The DC and RF sputtered films showed large crystals (>100 nm) without a predominant orientation, such large crystals induce enough surface roughness so that the films do not look shiny but opaque. On the other hand, the low energy PLD films were shiny and very smooth, so it was difficult to obtain good SEM pictures at higher amplifications. Such smoothness is typical of highly oriented films presenting what is called a fiber texture [56,57].

## 4. Discussion

Important materials properties, such as remnant polarization, dielectric constants, electronic transport and elastic moduli, are typically anisotropic, therefore, controlling the texture of the film is a key parameter for their applications. For this, it is important to identify the conditions leading to texture in the specific thin film material, so to understand the mechanism responsible for the development of the texture growth. The present paper compared the crystallographic orientation obtained for Bi thin films deposited using three different deposition methods; evaporation, sputtering and laser ablation. The changes in the crystallographic preferred orientation were analyzed as a function of the film thickness, which is greatly defined by the time-length of the deposition.

The results have shown that the Bi thin films presented either random or textured crystalline microstructures, where in textured samples there is a preferred growth plane parallel to the substrate. Although not a careful texture analysis was done, for example, measuring Pole figures, just by looking the normalized XRD patterns and the value of the $TC_{(003)}$ coefficient, it is possible to envision some of the most relevant deposition parameters involved in the texturing of the Bi films. One of these parameters is clearly the energy deposited at the growing film, administrated either by the energy of the impinging species or by the induced-substrate temperature. The texture (preferred orientation) in thin films can be thermodynamically and/or kinetically driven and not necessarily the final texture is the same. From the thermodynamic point of view, the texture (in non-epitaxial growth conditions) can be achieved when the properties of the individual crystals depend on the crystallographic directions or the shape of the crystals. The origin of texture in thin films can be classified as [58]: activated nucleation texture

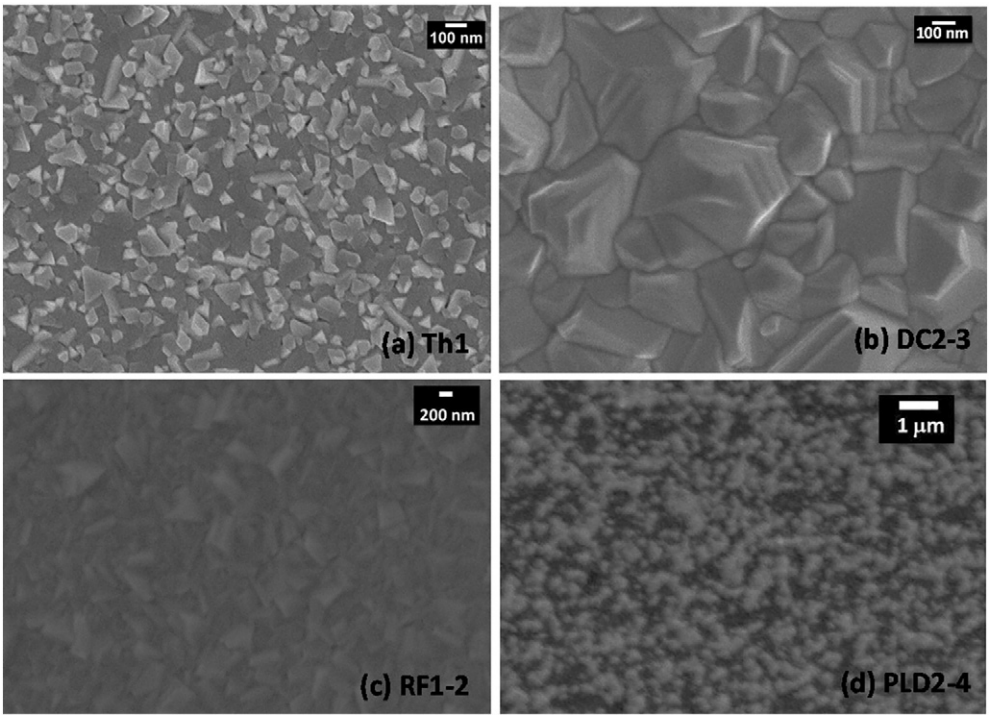


**Fig. 7.** SEM pictures showing the large differences in the films microstructure as a consequence of the preferred orientation (a) Thermal evaporated film showing a clear (003) preferred orientation, the triangular shape correspond to the projected view of the (003) planes. (b) DC-sputtered sample showing large Bi crystals. (c) RF-sputtered samples showed slightly smaller crystals and (d) PLD-HE (high energy) sample which shows a granular structure.

or evolutionary growth texture; the latter can be divided into restructuration or competitive growth. The mechanisms responsible for the texture include surface diffusion and grain boundary migration, which both strongly depend on the substrate temperature, angle of incidence of the species, impurities and surface-energy-driven recrystallization. On the other hand, the texture obtained by kinetic factors depends on differences in the deposition and growth rates of certain facets, which actually depend on the relative sticking coefficients [59]. On the other hand, energy-driven process such as ion bombardment which provides energy to increase the chemical reactivity between adatoms and the substrate, can also affect the texture by modifying the bonding and therefore the energetics of the growth process [59]. However, these parameters are not easy to determine and so the further analysis is presented in terms of the experimentally controlled conditions.

From Fig. 6, it could be argued that the change in the preferred orientation is related to the films thickness, as has been observed for metal nitrides [60]. However, for the E-beam sample, the $TC_{(003)}$ texture predominated even for thick samples, so we think that the variation in texture for the sputtered films is related to the heating of the substrate due to the longer deposition times, while a different mechanism define the texture in the PLD films.

Since different authors have shown that during deposition of Bi films, the primary Bi crystals are randomly oriented [53,61] and the fact that texture develops even on amorphous substrates; the mechanism of texture cannot be explained in terms of activated growth. During the competitive growth texture; initially a random orientation of the crystals is formed, however when the coalescence stage is reached and if the substrate temperature is below 0.3 $T_m$ ($T_m$ is melting point of the material, 271.4° for Bi), then competitive growth of certain orientation is established. The driving force is to achieve the minimum energy by preferentially growing the crystals which have the lowest surface energy crystal facet parallel to the substrate. Therefore, there is a preferred migration of adatoms to the low surface energy face [58,62,63]. Typically, for lamellar structures, like the rhombohedral Bi phase, the plane of minimum energy is indeed the basal plane, so this could explain that during low energetic deposition growth condition, the films showed the (003) preferred orientation. On the other hand, reconstruction growth occurs at higher growing energies (substrate temperature above 0.4 $T_m$, or high deposition rates or high ion energies); according to Lee [62], the deposit assumes the orientation that places the higher surface energy facets or the orientations with the faster growth rate parallel to the substrate. This surface correspond to the (120) or (012) planes in the hexagonal systems. However, Adamik et al. [58] describes this reconstruction growth texture as a consequence of the grain boundary migration, which allows certain orientation to grow laterally at the expenses of the others, such phenomena requires energies above a certain threshold.

Evaporation is the less energetic deposition method of the three systems. During evaporation, the atoms are ejected from the solid phase at low energies and at the point they arrive to the substrate, they have been completely thermalized. Thermal evaporation provides energy in the 0.1–0.25 eV. Under these conditions, a large preferred (003) orientation was observed for the thin films, even when relative thick samples were produced. Moreover, during evaporation, the substrates are essentially unheated and the maximum temperature attained by the substrate due to the radiation from the source is about 50–100 °C [64]. This explains that most of the evaporated thin films without substrate heating present a predominant (003) texture and nevertheless, the fast growth leads to rough films with average roughness around 20 nm and peak-to-peak exceeding 100 nm, as has been shown by Kokorian et al. [37], who were looking for an interesting application based on the one of the unique properties of Bi. Bi has the largest diamagnetic constant of all elements and at the micro-scale (200–500 nm thick) Bi thin films could be used for diamagnetic levitation in micromechanical systems. However, the roughness needs to be reduced to average values below 0.5 nm.

On the other hand, in magnetron sputtering, it has been shown that the neutral atoms ejected from the cathode have energies in the 0–20 eV range [64]. These atoms are expulsed with an excess kinetic energy and depending on the pressure and plasma conditions, they are usually arriving at the substrate at energies between 0.1 and 5 eV. For such

system, it was observed that the film structure showed a major preferred (003) orientation at low thickness (<200 nm) but as the thickness increased, the structure changed to a more random orientation showing (012), (003) and (104) peaks. It is also important to take into account that sputtering is well-known for the strong substrate heating caused as a consequence of the impingement of the growing species, but also of the recoiled Ar ions to the substrate. Therefore the strong dependence between the orientation and the thickness for the sputtered samples could be related to an increment in the substrate temperature as the thickness was increased; i.e. longer deposition times. The substrate temperature was not measured during these experiments, but previous analysis indicated that substrate can easily reach 150–250 °C. These temperature values mean that the homologous temperatures ($T_{substrate}/T_m$) for Bi deposition are in the 0.5–0.9 range, where strong changes in the microstructure can be produced. Moreover, such high homologous temperatures correspond to a high energy source for the adatoms, so that there is no longer need to retain the minimum equilibrium conditions. Stanley et al. [45] have measured the electrical transport properties of Bi films deposited by pulsed DC sputtering finding that the sheet resistance depend on the film structure, i.e. the texture. In good agreement with the present paper, they found that the (012) orientation was promoted as the film thickness increased above 200 nm from a range between 20 and 500 nm and also when substrate temperature was above 125 °C, while the (111) orientation was predominant (but not as strong as in evaporated films) at lower thicknesses and substrate temperatures, other more complexes correlations were found for the sputtering power and deposition pressure. An interesting feature that has been observed only on Bi films grown by sputtering is the formation of Bi whiskers [38,65], which appears as an interesting method to produce high quality Bi nanowires. Another interesting application of the Bi films produced by sputtering is as an electrochemical sensor to detect heavy metals in water [66], substituting the mercury electrodes commonly used.

In evaporation and sputtering, most of the film-growing species are neutral atoms and not ions. Meanwhile, for the PLD system, most of the species arriving at the substrate are energetic ions. As described in the deposition conditions, the energy of such ions can be changed and controlled in a range (100 to 300 eV), which is much higher than for sputtering or evaporation. Therefore, the texture attained by PLD is more probably energetically-driven instead of thermodynamically. Nevertheless, despite the higher energy of the ions for the PLD-LE conditions in comparison to the other deposition techniques, the results indicated that the films grew oriented in the (003) direction independently of the thickness and therefore the deposition time. For PLD, substrate heating is not a problem and despite the energy-input from the ions, the film texture was the (003), i.e. the minimum surface energy facet. The texture was obtained through a competitive growth mechanism and the ion energy served as a source for adatom mobility, which will also explain that the PLD films were smoother than the evaporated or sputtered films (data not shown), but the energy deposited at the substrate was not enough to allow the growth along other directions.

At the high energies (~280 eV), the PLD films did not show a (003) texture since the maximum $TC_{(003)}$ coefficient was about 2.3 and it decreased drastically as the thickness increased from 60 to 200 nm. Finally, for the thicker film (800 nm) the (012) direction was predominant. Since again there is not substrate heating, this change must be related to the energy-enhanced growth of the films. It is possible that a restructuration growth mechanism is established since the grain boundaries have enough mobility induced by the excess energy of the impinging ions.

Boffoue et al. [67] deposited Bi films using PLD and reported a change in the preferred orientation from (012) for discontinuous films with thickness below 26 nm to the (003) for the continuous and thicker films. However, no information about the ion energy is provided. Dauscher et al. [43] reported strong variations in the texture of Bi thin films deposited by PLD as a consequence of the substrate or post-annealing temperature. Their results indicated that the (012) texture is obtained when the temperature is increased in agreement with the idea that more energetic growth conditions are required to obtain the (012) preferential growth. Toudert et al. [33] used the PLD deposited Bi thin films oriented along the (003) orientation to determine properly the optical properties of Bi films without changing the deposition conditions or film thickness. Moreover, for this group, calculation of the optical properties for the (012) oriented films might be interesting. On the other hand, Yao et al. [68] demonstrate the efficiency of the PLD-deposited Bi films as an ultra-broadband and high responsive detector. In that work, the films thickness was varied from 100 to 600 nm and a drastic change in the photocurrent was observed around 240 nm, which is explained in terms of the topological insulator properties of the films. However, nothing is mentioned about the effect that the film texture might have on the conductivity; only the diffraction patterns from samples thinner than 240 nm are shown, showing (003)-oriented films. However, the degree of texture is slightly lower than that the PLD-LE films, since the (012) reflection is also observed. If their deposition conditions are similar to those used in the present paper, then the results indicate that the (003) orientation might be retained for Bi thickness up to 600 nm.

## 5. Conclusion

Bismuth thin films with thickness ranging from a few nanometers to 2 μm were deposited by DC and RF sputtering; thermal and electron-beam evaporation and pulsed laser deposition. The analyses of the XRD data suggest that films presenting a predominantly preferred orientation with the c-axis of the hexagonal crystal perpendicular to the substrate, i.e. (003) preferred orientation can be achieved by limiting the energy supplied to the growth process. For the PLD deposition, this could be achieved by selecting the ion energy of the impinging ions; values below 120 eV lead to (003) orientation independently of the film thickness. Similarly, both electron-beam and thermal evaporation, which are intrinsically low energy deposition systems, were able to produce (003) oriented films within a large range of thicknesses. On the other hand, the sputtering method produced significant heating of the substrate and such increment in the homologous temperature tends to produce randomly oriented crystals. Finally, we have demonstrated that PLD films presenting a nearly 100% (012) orientation are possible by setting the ion energy of the impinging ions about 270 eV.

The development of the (003) texture on the Bi thin films is explained in terms of the competitive growth texture in which the lowest energy crystal facets grow faster than the others. Meanwhile for the (012) growth, the mechanism is more probably restructuring growth texture, dominated by a large mobility of the grain boundaries as a consequence of the energy provided by the impinging ions.

## Funding sources

This work was supported by the European Union FP7-NMP EU-Mexico programme under grant agreement no 263878 and by CONACYT no 125141. Acknowledgements to DGAPA-PAPIIT (IN100116) and CONACYT (251279) for funding projects.

## References

[1] M.R. Neuman, W.H. Ko, Structure determined electrical transport properties of bismuth thin films, J. Vac. Sci. Technol. 3 (1966) 314.
[2] J.Y. Letraon, H.A. Combet, Electrical conductivity and halls effect of bismuth thin films between 4.2 degrees Kelvin and 300 degrees Kelvin, J. Phys. Paris 30 (1969) 419.
[3] M. Monsion, M. Massenat, Measuring photoelectromagnetic effect in bismuth thin films, C.R. Acad. Sci. B Phys. 268 (1969) 1671.
[4] V.V. Andrievs, Y.F. Komnik, Magnetoresistance of Bismuth Thin Films in a Parallel Magnetic Field, Sov. Phys. Solid State 12 (1970) 1254.

[5] D.L. Miller, G.I. Moller, Quantum size effects in polycrystalline bismuth thin films, Am. J. Phys. 39 (1971) 567–568.
[6] V.I. Burchako, D.V. Gitsu, M.I. Kozlovsk, Some peculiarities of thermo emf in bismuth thin-films, Fiz. Tverd. Tela 14 (1972) 907.
[7] A.I. Usoskin, I.N. Shklyare, A.S. Gerchiko, Y.S. Verlinsk, Optical properties of bismuth thin-films, Opt. Spektrosk. 34 (1973) 954–958.
[8] P. Mikolajc, W. Piasek, M. Subotowi, Thermoelectric-power in bismuth thin-films, Phys. Status Solidi A 25 (1974) 619–628.
[9] C.A. Hoffman, J.R. Meyer, F.J. Bartoli, A. Divenere, X.J. Yi, C.L. Hou, H.C. Wang, J.B. Ketterson, G.K. Wong, Semimetal-to-semiconductor transition in bismuth thin-films, Phys. Rev. B 48 (1993) 11431–11434.
[10] T. Flores, M. Arronte, E. Rodriguez, L. Ponce, J.C. Alonso, C. Garcia, M. Fernandez, E. Haro, Bismuth thin films obtained by pulsed laser deposition, P. Soc. Photo-Opt. Ins. 3572 (1999) 70–73.
[11] K.I. Lee, M.H. Jeun, J.M. Lee, J.Y. Chang, S.H. Han, J.G. Ha, W.Y. Lee, Magnetotransport properties in semimetallic bismuth thin films, Mater. Sci. Forum 449–4 (2004) 1061–1064.
[12] A.D. Liao, M.L. Yao, F. Katmis, M.D. Li, S. Tang, J.S. Moodera, C. Opeil, M.S. Dresselhaus, Induced electronic anisotropy in bismuth thin films, Appl. Phys. Lett. 105 (2014), 063114. .
[13] A. Takayama, High-resolution Spin-resolved Photoemission Spectrometer and the Rashba Effect in Bismuth Thin Films, Springer Theses-Reco, 2015 1–83.
[14] D. Lukermann, S. Sologub, H. Pfnur, C. Tegenkamp, Sensing surface states of Bi films by magnetotransport, Phys. Rev. B 83 (2011) 245425.
[15] V.D. Das, N. Soundararajan, Size and temperature effects on the Seebeck coefficient of thin bismuth-films, Phys. Rev. B 35 (1987) 5990–5996.
[16] E.I. Rogacheva, S.N. Grigorov, O.N. Nashchekina, S. Lyubchenko, M.S. Dresselhaus, Quantum-size effects in n-type bismuth thin films, Appl. Phys. Lett. 82 (2003) 2628–2630.
[17] H.T. Chu, W. Zhang, Quantum size effect and electric-conductivity in thin-films of pure bismuth, J. Phys. Chem. Solids 53 (1992) 1059–1065.
[18] M. Bianchi, F. Song, S. Cooil, A.F. Monsen, E. Wahlstrom, J.A. Miwa, E.D.L. Rienks, D.A. Evans, A. Strozecka, J.I. Pascual, M. Leandersson, T. Balasubramanian, P. Hofmann, J.W. Wells, One-dimensional spin texture of Bi(441): quantum spin Hall properties without a topological insulator, Phys. Rev. B 91 (2015) 165307.
[19] Lecontel, J.Y. Letraon, H.A. Combet, Quantum size effects in elastoresistance of bismuth thin films, J. Phys. Paris 32 (1971) 553.
[20] J.M. Guerra, M.S. Balmaseda, Observation of a size effect in laser-induced thermomagnetic potentials in bismuth thin-films, Phys. Rev. B 33 (1986) 3745–3748.
[21] S. Condurache-Bota, R. Drasovean, N. Tigau, A.P. Rambu, The influence of substrate temperature on the structure and on the optical reflection spectrum of bismuth thin films, Rev. Roum. Chim. 56 (2011) 1101–1106.
[22] M. Rudolph, J.J. Heremans, Electronic and quantum phase coherence properties of bismuth thin films, Appl. Phys. Lett. 100 (2012) 241601.
[23] F. Pang, X.J. Liang, Z.L. Liao, S.L. Yin, D.M. Chen, Origin of the metallic to insulating transition of an epitaxial Bi(111) film grown on Si(111), Chin. Phys. B 19 (2010).
[24] H.T. Chu, Comment on "Semimetal-to-semiconductor transition in bismuth thin films", Phys. Rev. B 51 (1995) 5532–5534.
[25] K.S. Wu, M.Y. Chem, Temperature-dependent growth of pulsed-laser-deposited bismuth thin films on glass substrates, Thin Solid Films 516 (2008) 3808–3812.
[26] A.A. Ramadan, A.M. Elshabiny, N.Z. Elsayed, Size-dependent structural characteristics of thin bismuth-films, Thin Solid Films 209 (1992) 32–37.
[27] J.W. Wells, K. Handrup, J.F. Kallehauge, L. Gammelgaard, P. Boggild, M.B. Balslev, J.E. Hansen, P.R.E. Petersen, P. Hofmann, The conductivity of Bi(111) investigated with nanoscale four point probes, J. Appl. Phys. 104 (2008), 053717. .
[28] V.M. Grabov, E.V. Demidov, V.A. Komarov, Mobility restriction of charge carriers in bismuth films due to film block structure, J. Surf. Invest.: X-Ray, Synchrotron Neutron Tech. 5 (2011) 177–181.
[29] S. Golin, Band structure of bismuth: pseudopotential approach, Phys. Rev. 166 (1968) 643–651.
[30] M.H. Cohen, Energy bands in the bismuth structure. I. A nonellipsoidal model for electrons in Bi, Phys. Rev. 121 (1961) 387–395.
[31] G. Jezequel, J. Thomas, I. Pollini, Experimental band structure of semimetal bismuth, Phys. Rev. B 56 (1997) 6620–6626.
[32] J. Chang, H. Kim, J. Han, M.H. Jeon, W.Y. Lee, Microstructure and magnetoresistance of sputtered bismuth thin films upon annealing, J. Appl. Phys. 98 (2005).
[33] J. Toudert, R. Serna, I. Camps, J. Wojcik, P. Mascher, E. Rebollar, T.A. Ezquerra, Unveiling the far infrared-to-ultraviolet optical properties of bismuth for applications in plasmonics and nanophotonics, J. Phys. Chem. C 121 (2017) 3511–3521.
[34] K.S. Wu, M.Y. Chern, Electrical transport properties of n-type (110)-oriented bismuth thin films grown at 110 K on glass substrates, J. Appl. Phys. 104 (2008).
[35] R. Atkinson, P.H. Lissberger, Optical constants of thin film bismuth, Thin Solid Films 17 (1973) 207–221.
[36] R. Koseva, I. Monch, D. Meier, J. Schumann, K.F. Arndt, L. Schultz, B. Zhao, O.G. Schmidt, Evolution of hillocks in Bi thin films and their removal upon nanoscale mechanical polishing, Thin Solid Films 520 (2012) 5589–5592.
[37] J. Kokorian, J.B.C. Engelen, J. de Vries, H. Nazeer, L.A. Woldering, L. Abelmann, Ultra-flat bismuth films for diamagnetic levitation by template-stripping, Thin Solid Films 550 (2014) 298–304.
[38] S.A. Stanley, C. Stuttle, A.J. Caruana, M.D. Cropper, A.S.O. Walton, An investigation of the growth of bismuth whiskers and nanowires during physical vapour deposition, J. Phys. D. Appl. Phys. 45 (2012).
[39] Z.L. Bao, K.L. Kavanagh, Epitaxial Bi/GaAs(111) diodes via electrodeposition, Appl. Phys. Lett. 88 (2006).
[40] H. Hattab, E. Zubkov, A. Bernhart, G. Jnawali, C. Bobisch, B. Krenzer, A. Acet, R. Moeller, M.H.V. Hoegen, Epitaxial Bi(111) films on Si(001): strain state, surface morphology, and defect structure, Thin Solid Films 516 (2008) 8227–8231.
[41] F.Y. Yang, K. Liu, K.M. Hong, D.H. Reich, P.C. Searson, C.L. Chien, Large magnetoresistance of electrodeposited single-crystal bismuth thin films, Science 284 (1999) 1335–1337.
[42] B. O'Brien, M. Plaza, L.Y. Zhu, L. Perez, C.L. Chien, P.C. Searson, Magnetotransport properties of electrodeposited bismuth films, J. Phys. Chem. C 112 (2008) 12018–12023.
[43] A. Dauscher, A. Jacquot, B. Lenoir, Temperature dependent growth of pulsed laser deposited Bi films on BaF2(111), Appl. Surf. Sci. 186 (2002) 513–520.
[44] D.H. Kim, S.H. Lee, J.K. Kim, G.H. Lee, Structure and electrical transport properties of bismuth thin films prepared by RF magnetron sputtering, Appl. Surf. Sci. 252 (2006) 3525–3531.
[45] S.A. Stanley, M.D. Cropper, Structure and resistivity of bismuth thin films deposited by pulsed DC sputtering, Appl. Phys. Mater. Sci. Process. 120 (2015) 1461–1468.
[46] B. Doggett, J.G. Lunney, Langmuir probe characterization of laser ablation plasmas, J. Appl. Phys. 105 (2009), 033306. .
[47] N.M. Bulgakova, A.V. Bulgakov, O.F. Bobrenok, Double layer effects in laser-ablation plasma plumes, Phys. Rev. E 62 (2000) 5624–5635.
[48] G.B. Harris, X. Quantitative measurement of preferred orientation in rolled uranium bars, Lond. Edinb. Dublin Philos. Mag. J. Sci. 43 (1952) 113–123.
[49] M.P. Seah, W.A. Dench, Quantitative electron spectroscopy of surfaces: a standard data base for electron inelastic mean free paths in solids, Surf. Interface Anal. 1 (1979) 2–11.
[50] P. Van der Heide, X-ray Photoelectron Spectroscopy, an Introduction to Principles and Practices, Wiley, 2012.
[51] R. Atkinson, E. Curran, Ellipsometric examination of the oxidation of vacuum-deposited bismuth films, Thin Solid Films 128 (1985) 333–339.
[52] J.C.G. de Sande, T. Missana, C.N. Afonso, Optical properties of pulsed laser deposited bismuth films, J. Appl. Phys. 80 (1996) 7023–7027.
[53] V.M. Grabov, E.V. Demidov, V.A. Komarov, Atomic-force microscopy of bismuth films, Phys. Solid State 50 (2008) 1365–1369.
[54] M. Chen, J.-P. Peng, H.-M. Zhang, L.-L. Wang, K. He, X.-C. Ma, Q.-K. Xue, Molecular beam epitaxy of bilayer Bi(111) films on topological insulator Bi2Te3: a scanning tunneling microscopy study, Appl. Phys. Lett. 101 (2012), 081603. .
[55] A. Takayama, T. Sato, S. Souma, T. Oguchi, T. Takahashi, One-dimensional edge states with giant spin splitting in a bismuth thin film, Phys. Rev. Lett. 114 (2015), 066402. .
[56] P.B. Barna, M. Adamik, Fundamental structure forming phenomena of polycrystalline films and the structure zone models, Thin Solid Films 317 (1998) 27–33.
[57] P.B. Barna, Surface chemical phenomena and growth of films, Thin Solid Films 85 (1981) 263–264.
[58] M. Adamik, P.B. Barna, I. Tomov, D. Biro, Problems of structure evolution in polycrystalline films. Correlation between grain morphology and texture formation mechanisms, Phys. Status Solidi A 145 (1994) 275–281.
[59] D.L. Smith, Thin Film Deposition. Principles and Practice, McGraw-Hill, 1995.
[60] W.D. Sproul, P.J. Rudnik, M.E. Graham, The effect of N2 partial pressure, deposition rate and substrate bias potential on the hardness and texture of reactively sputtered TiN coatings, Surf. Coat. Technol. 39–40 (Part 1) (1989) 355–363.
[61] J. Berty, M. Brieu, M.J. David, L. Lafourcade, P. Larroque, Structural evolution of bismuth thin-films between 8 K and 573 K - effect of supercooling, Thin Solid Films 60 (1979) 97–104.
[62] D.N. Lee, A model for development of orientation of vapour deposits, J. Mater. Sci. 24 (1989) 4375–4378.
[63] K. Wasa, M. Kitabatake, H. Adachi, Thin Film Materials Technology: Sputtering of Compound Materials, William Andrew, Inc. and Springer-Verlag GmbH & Co. KG, 2004.
[64] S. Middleman, A. Hochberg, Process Engineering: Analysis in Semiconductor Device Fabrication, Mcgraw-Hill College, 1993.
[65] S. Cao, C. Guo, Y. Wang, J. Miao, Z. Zhang, Q. Liu, Template-catalyst-free growth of single crystalline bismuth nanorods by RF magnetron sputtering method, Solid State Commun. 149 (2009) 87–90.
[66] J. Baron, P. Silva-Bermudez, S.E. Rodil, Sputtered Bismuth thin films as trace metal electrochemical sensors, MRS Proc. 1477 (2013).
[67] M.O. Boffoue, B. Lenoir, A. Jacquot, H. Scherrer, A. Dauscher, M. Stolzer, Structure and transport properties of polycrystalline Bi films, J. Phys. Chem. Solids 61 (2000) 1979–1983.
[68] J.D. Yao, J.M. Shao, G.W. Yang, Ultra-broadband and high-responsive photodetectors based on bismuth film at room temperature, Sci Rep 5 (2015) 12320.